

# U-Pb zircon and titanite geochronological constraints on the late/post-Caledonian evolution of the Scandinavian Caledonides in north-central Norway

Øystein Larsen, Øyvind Skår & Rolf-Birger Pedersen

Larsen, Ø., Skår, Ø. & Pedersen, R.-B.: U-Pb zircon and titanite geochronological constraints on the late/post-Caledonian evolution of the Scandinavian Caledonides in north-central Norway. *Norsk Geologisk Tidsskrift*, Vol 82, pp. 1-13. Trondheim 2002, ISSN 029-196X.

U-Pb geochronology and structural investigations in coastal areas of the north-central Norwegian Caledonides indicate different responses to late/post-Scandian tectono-thermal events in the east (the Sjøna window) and west (the island of Træna). The earliest event in the Sjøna window involved migmatite formation associated with high-grade metamorphism at around 425 Ma. Associated structures indicate that this event was related to Scandian east-directed thrusting. A metamorphic event of similar age ( $424 \pm 6$  Ma) is recorded on Træna, but the structural response to the thrusting was insignificant as compared to the Sjøna window. During and/or following nappe emplacement, the Sjøna window evolved into a dome structure. Ductile non-coaxial shearing apparently associated with this dome formation affected granitic pegmatites dated to  $409 \pm 5$  Ma. The emplacement of these Early Devonian pegmatites in the Sjøna window overlapped with the formation of migmatites and pegmatites on Træna at  $398 \pm 2$  Ma and  $403 \pm 3$  Ma, respectively. In contrast to the Sjøna window, however, the migmatites and pegmatites on Træna are interpreted to be coeval with ductile, bulk coaxial deformation characterized by sub-vertical shortening and E-W extension. Titanite associated with mineralized normal faults on Træna yields an age of  $368 \pm 6$  Ma, indicating that rocks on Træna had been exhumed into the brittle regime by Middle-Late Devonian time. Semi-brittle to brittle deformation in the Sjøna window is suggested to be of Middle Devonian-Early Carboniferous age on the basis of other radiometric dating. It is inferred that the rocks on Træna were situated at deeper crustal levels than their equivalents in the Sjøna window in the Late Silurian-Early Devonian (c. 425 to 400 Ma). In the following (c. 400-370 Ma), however, differential exhumation resulted in juxtaposition of these two areas at approximately similar crustal levels.

Øystein Larsen<sup>1</sup>, Øyvind Skår<sup>2</sup> & Rolf B. Pedersen, Department of Geology, University of Bergen, Allégt. 41, N-5007 Bergen. <sup>1</sup> Present address: Statoil, Sandslihaugen 30, 5020 Bergen, <sup>2</sup> Present address: Norges geologiske undersøkelse, 7491 Trondheim, Norway.

## Introduction

The final closure of the Iapetus Ocean and continental collision in the Late Silurian to Early Devonian resulted in E- to SE-directed nappe emplacement onto the Baltic margin. This contractional stage, commonly referred to as the Scandian event (Gee 1975; Roberts & Gee 1985), was closely followed and partly overlapped by extensional reworking of the orogenic crust under ductile to progressively more brittle conditions. The contractional and extensional evolution of the orogen has been extensively studied in southwest Norway (e.g. Andersen & Jamtveit 1990; Fossen 1992; Milnes et al. 1997; Fossen & Dunlap 1998) and in the Lofoten-Ofoten area of north Norway (Rykkeliid & Andresen 1994; Coker et al. 1995; Northrup 1996, 1997; Klein et al. 1999; Klein & Steltenpohl 1999). However, less attention has been paid to the relationship between contraction and extension in the Caledonides of north-central Norway. We present U-Pb zircon and titanite ages combined with field observations from this area, which provide constraints on the late/post-Scandian deformation and metamorphism.

## Tectonic setting

The structurally lowest unit(s) in the Caledonian tectonostratigraphy of the north-central Norwegian coast, where the present study was carried out (Fig. 1), mostly comprise granitic gneisses. These rocks are by most workers interpreted as part of the parautochthonous basement, but may alternatively be interpreted as part of the allochthon (Stephens et al. 1985; Osmundsen et al. in press). The granitic gneisses typically occur in tectonic windows (e.g. the Sjøna window), defining culminations that affect the overlying Caledonian nappes. The formation of these gneiss-cored culminations is controversial and has been ascribed to different processes, at different stages in the orogenic evolution. In general, the proposed models include contractional, gravitational and extensional tectonics (e.g. Ramberg 1980; Greiling et al. 1993; Rykkeliid & Andresen 1994). The Caledonian nappes overlying the tectonic windows include (from bottom to top) the Rödingsfjället and Helgeland Nappe Complexes (RNC and HNC, Fig. 1) with rocks exotic to Baltica (Stephens et al. 1985). These rocks, mostly consisting of garnet-mica schist

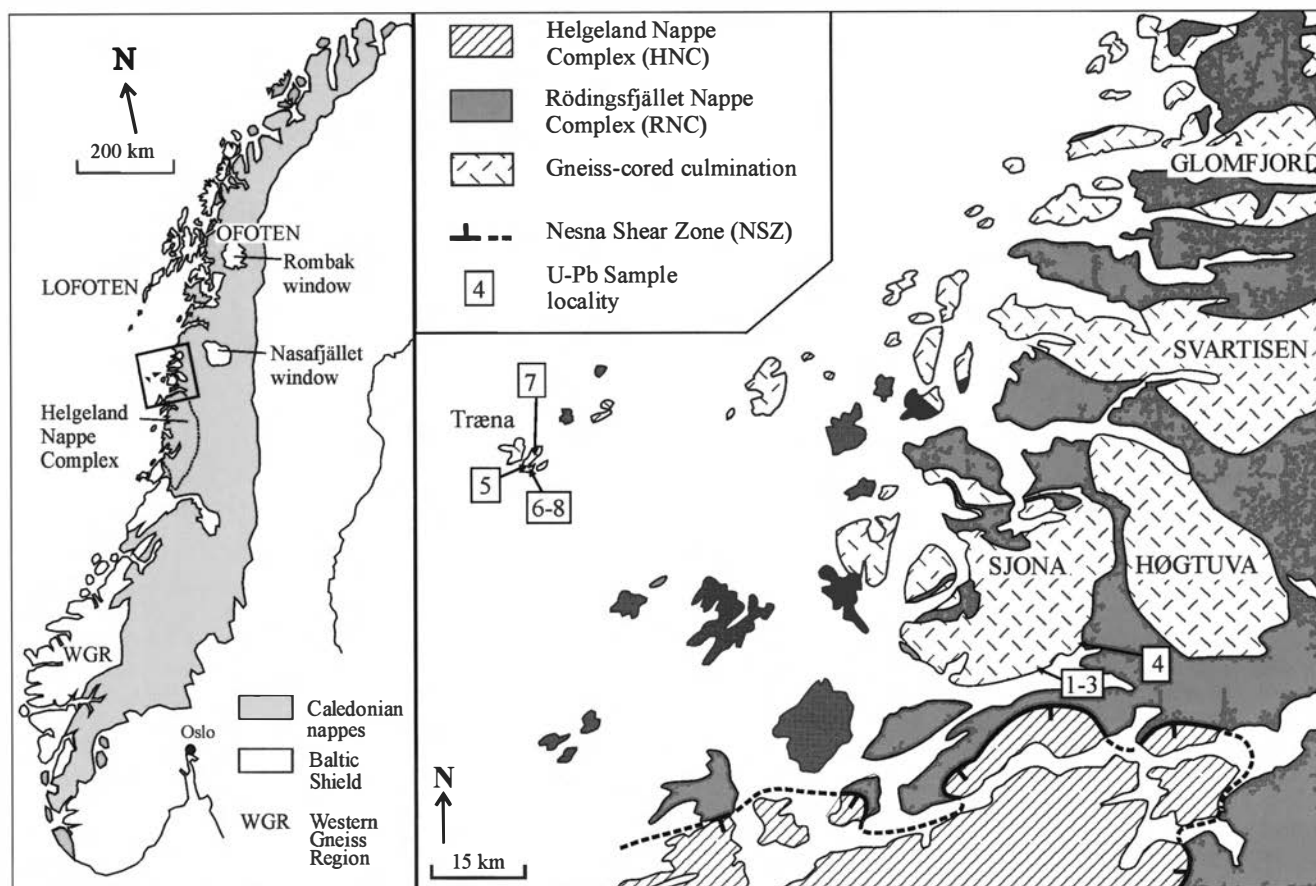


Fig. 1. Simplified geological maps. Left: the Scandinavian Caledonides with locations of areas referred to in the text. Right: the main tectonic units in north-central Norway (modified from Gustavson & Gjelle 1991) with locations of U-Pb samples analysed in this study. The location of the Nesna shear zone is adopted from Osmundsen et al. (in press).

(RNC) and various granites, marbles and mica schists (HNC) (Gustavson & Gjelle 1991), preserve the highest tectonostratigraphic levels in the Scandinavian Caledonides, the Uppermost Allochthon (Roberts & Gee 1985).

This study was carried out along the southern margin of the Sjøna window, one of the gneiss-cored culminations mentioned above, and on the island of Træna some 50 km westward (Fig. 1). The rocks in these two areas formed at around 1800 Ma (e.g. Wilson & Nicholson 1973; Skår 2002), and are probably influenced by a long and complex deformation history. Nevertheless, age determinations in this study indicate that a substantial part of the ductile deformation was late Silurian to Early Devonian in age.

In contrast to southwest Norway and the Lofoten/Ofoten area of north Norway, evidence for regional extensional reworking of the Caledonides has until recently not been documented in north-central Norway. The contact between RNC and HNC, however, is now interpreted as a major extensional, ductile shear zone, the Nesna Shear Zone (NSZ), with top-to-the-WSW displacement (Fig. 1; Osmundsen et al. in press). The southern margin of the Sjøna window is located in the

footwall of the NSZ, structurally some 2–3 km below the base of the HNC. It is therefore likely that ductile deformation in the NSZ influenced the structural development in the Sjøna window.

#### Previous geochronology

Around 100 km to the south of the present study area, the youngest intrusion of the Bindal Batholith, confined to the HNC, was dated by the U/Pb method on zircon to  $430 \pm 7$  Ma (Nordgulen et al. 1993). Since the intrusion predates Scandian deformation, this age also provides a maximum age for Scandian thrusting in the area. This age is in accordance with time constraints based on Llandoveryan fossils further east (e.g. Gee 1975). Furthermore, syn-kinematic intrusions and metamorphic minerals from the same tectonostratigraphic level (the Uppermost Allochthon) in the Ofoten area of northern Norway (Fig. 1) yield U/Pb ages of ca. 430 Ma (Coker et al. 1995; Northrup 1997), interpreted to date Scandian metamorphism and east-directed thrusting.

A brief review of radiometric age determinations from gneiss-cored culminations in north-central Norway is

presented below. Dallmeyer (1988) reported  $^{40}\text{Ar}/^{39}\text{Ar}$  amphibole ages of 418–401 Ma from the Sjona and Høgtuva windows, which reflect cooling through 500°C. In the Høgtuva window, Wilberg (1987) reported younger Rb/Sr whole-rock biotite ages of around 350 Ma, which were interpreted to date cooling of these rocks to around 350°C. However,  $^{40}\text{Ar}/^{39}\text{Ar}$  biotite ages between  $384 \pm 1$  and  $378 \pm 1$  Ma in the Sjona window suggest that this temperature was reached earlier (Eide et al. in review). Wilson & Nicholson (1973) reported mean Rb/Sr whole-rock biotite ages of 350 Ma and 380 Ma from the Glomfjord and Nasafjället windows, respectively (Fig. 1) (ages recalculated to a decay constant of  $1.42 \times 10^{-11}/\text{y}$ , Steiger & Jäger 1977). Essex & Gromet (2000) presented U/Pb ages of metamorphic titanites from the western margin of the Nasafjället window. These ages fall into an early prograde and a late retrograde group, interpreted in terms of subduction of the Baltic margin (417–399 Ma) followed by a phase of exhumation during late Scandian contraction (401–386 Ma).

At present, the only existing radiometric dating from the NSZ includes  $^{40}\text{Ar}/^{39}\text{Ar}$  white mica and biotite ages that fall between  $398 \pm 1$  and  $387 \pm 1$  Ma, interpreted to date top-to-the-WSW shearing (Eide et al. in review; Osmundsen et al. in press). Thus, the ductile extensional deformation in the NSZ appears to be broadly coeval with the youngest  $^{40}\text{Ar}/^{39}\text{Ar}$  amphibole ages of Dallmeyer (1988) from the Sjona and Høgtuva windows, and the retrograde group of U/Pb titanite ages reported by Essex & Gromet (2000) from the Nasafjället window.

## The Sjona window

The present investigation in the Sjona window is concentrated along the southern margin (Fig. 2). This part of the window predominantly comprises granitic gneiss, with minor amounts of mafic rocks. These rocks are heterogeneously deformed, ranging from weakly deformed augen gneisses (L-tectonites) to highly sheared mylonites (LS-tectonites). The latter are particularly well developed along the eastern contact to the overlying RNC (Fig. 2). The gneisses also contain minor amounts of migmatites and discordant granitic pegmatites, whose deformed remnants partly define the foliation, and therefore represent important time markers.

### Structural relationships

The foliation trends in the Sjona window and the overlying allochthons are generally concordant and define a sub-circular dome structure that resembles other gneiss-cored culminations in central and northern Norway. In the southeastern part of the Sjona window, the foliation dips ESE, gradually changing towards the

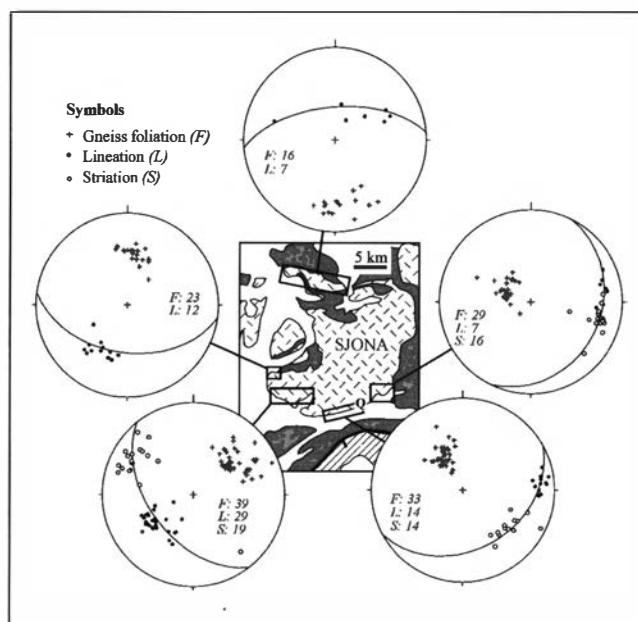


Fig. 2. Stereoplots (equal area lower hemisphere projection) showing structural variations across the Sjona window (figure 1 for legend). Great circles are the mean foliation orientations. Letters F, L and S refer to the number of measurements of the main foliation (poles), stretching lineation and semi-brittle to brittle shear zone striation, respectively. Q on the map shows the location of the quarry from which samples 1–3 were collected (see text for details).

SE in the south, and to the SW and SSW in the southwest (Fig. 2). In the northern part of the window, a less well defined foliation dips N to NW. The stretching lineation associated with the gneiss foliation plunges E in the south and southeast, accompanied by top-to-the-E structures (Fig. 3a), and plunges SW in the southwest, accompanied by top-to-the-SW structures (Fig. 3b). A few measurements in the north show a lineation plunging mostly N to NE. Thus, a roughly radial pattern is depicted by these structures. This pattern is also recorded by asymmetric structures in the RNC just above the nappe contact, indicating shearing after the nappe emplacement.

Important relationships between deformational and thermal events are provided in a quarry in the southern part of the Sjona window (Fig. 4a). At this locality, migmatite neosomes are sheared into layers parallel to the gneiss foliation (Fig. 4b). The migmatite formation was therefore pre- or syn-tectonic with respect to development of the amphibolite-facies fabric in the gneiss and top-to-the-E shearing. In the same quarry, veins of granitic pegmatites cut and post-date the foliation (Fig. 4a). Although largely undeformed, these pegmatites do show some minor folding with foliation-parallel axial surfaces, reflecting a later stage of ductile deformation. Southwest in the Sjona window, similar granitic pegmatites appear to be slightly overprinted by the top-to-the-SW shearing, suggesting that these structures formed at the same time.

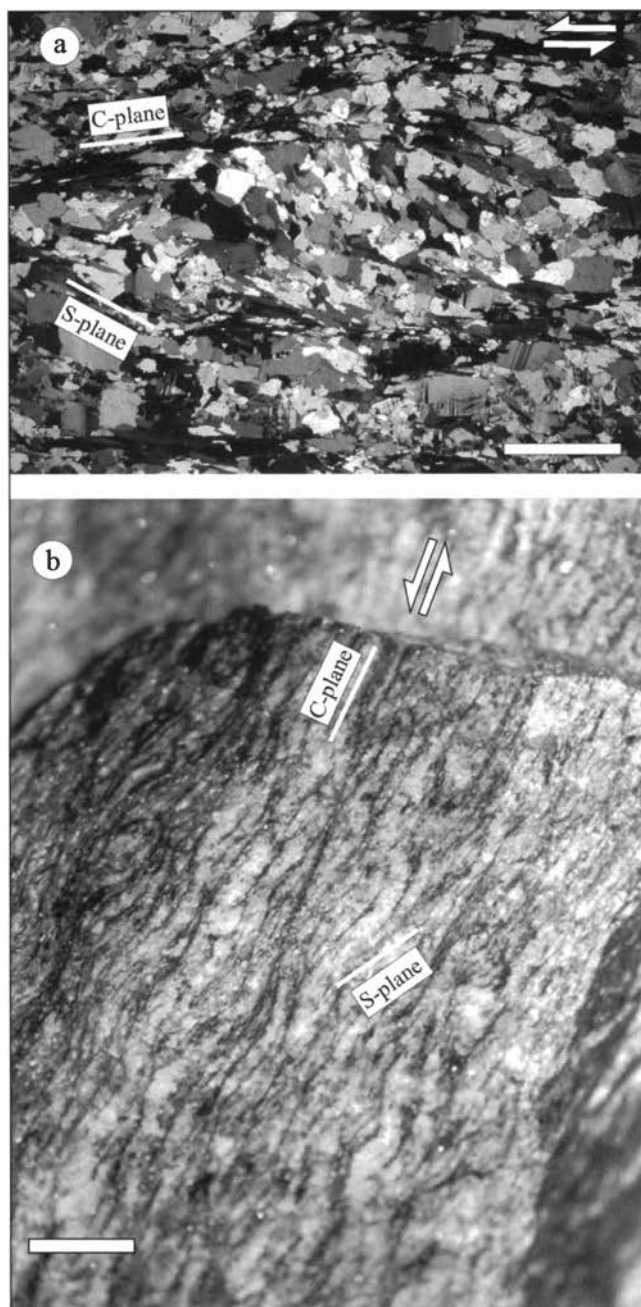


Fig. 3. a) Microphotograph (crossed polars) showing C-S fabric defined by amphibolite facies minerals and consistent with top-to-the-E shear near the E margin of the Sjøna window. Scale bar is 2 mm. b) C-S fabric defined by amphibolite facies minerals and consistent with top-to-the-SW shear in the SW part of the window, seen towards NW. The C-planes correspond to the main foliation and contain the SW-plunging stretching lineations. Scale bar is 2 cm.

Following the ductile deformation described above, semi-brittle to brittle deformation resulted in shearing along discrete surfaces parallel to the gneiss foliation (Fig. 4c). These discrete shear zones are coated with polished and striated chlorite and sericite, reflecting retrograde replacement of biotite and feldspar under greenschist-facies conditions. The plunge azimuth of the striation is at variance with the earlier described stret-

ching lineation, and changes across the dome (Fig. 2). In the southern and southeastern part of the Sjøna window, the striation plunges SE and ESE. The displacement here is dominated by extensional dip-slip, as seen in the above-mentioned quarry (Fig. 4c). In contrast, the striations plunge NW in the southwest, implying a more strike-slip dominated displacement along the foliation (Fig. 2 and 5). Unfortunately, we were not able to determine the sense of shear in the latter area. However, based on the extensional nature of the deformation to the east, a component of normal displacement may reasonably be assumed, which would imply a component of dextral shear in this part of the window. Asymmetric folds with top-to-the-NW vergence reported from the weaker garnet-mica schist of the overlying RNC (Osmundsen et al., in press) are in agreement with this assumption. If correct, kinematic analysis indicates that the semi-brittle to brittle shear zones formed under approximately E-W extension and vertical shortening, provided that their initial orientation is preserved (Fig. 5).

## The islands of Træna

Comparable lithologies and protolithic ages suggest that the rocks of Træna correlate with those in the Sjøna window (Skår 2002). Træna mostly comprises granitic gneiss surrounding a body of mafic rock in central parts of the island (Fig. 6). The latter alternates between anorthositic and amphibolitic rocks. Some lenses of garnet amphibolite contain symplectites of amphibole and plagioclase that are characteristic for rocks formed by retrograde metamorphism of eclogites (Krogh 1980). In contrast to the Sjøna window, no contacts to the allochthons are exposed on Træna. Allochthonous rocks are exposed on small islands around 5 km to the north; however, the contact to these rocks is probably defined by post-Caledonian faults located in the sea (Fig. 1, Gustavson & Gjelle 1991).

### Structural relationships

The gneisses on Træna have a well-developed foliation that dips 10–30° N (Fig. 6). In contrast to the Sjøna window, a weak and inconsistently oriented lineation is associated with the foliation in most parts of Træna. Although a WNW-plunging lineation associated with top-to-the-ESE shearing is reported along the southeast coast (Osmundsen et al. in press), the gneiss on Træna generally classifies as an S-tectonite. The foliation of the mafic rocks is mostly concordant to the gneiss foliation. However, remnants of an older, discordant foliation are locally exposed, which is reflected by a more scattered distribution of foliation poles as compared to the surrounding gneiss (Fig. 6). Generally, the mafic rocks therefore appear to be less deformed than the fel-

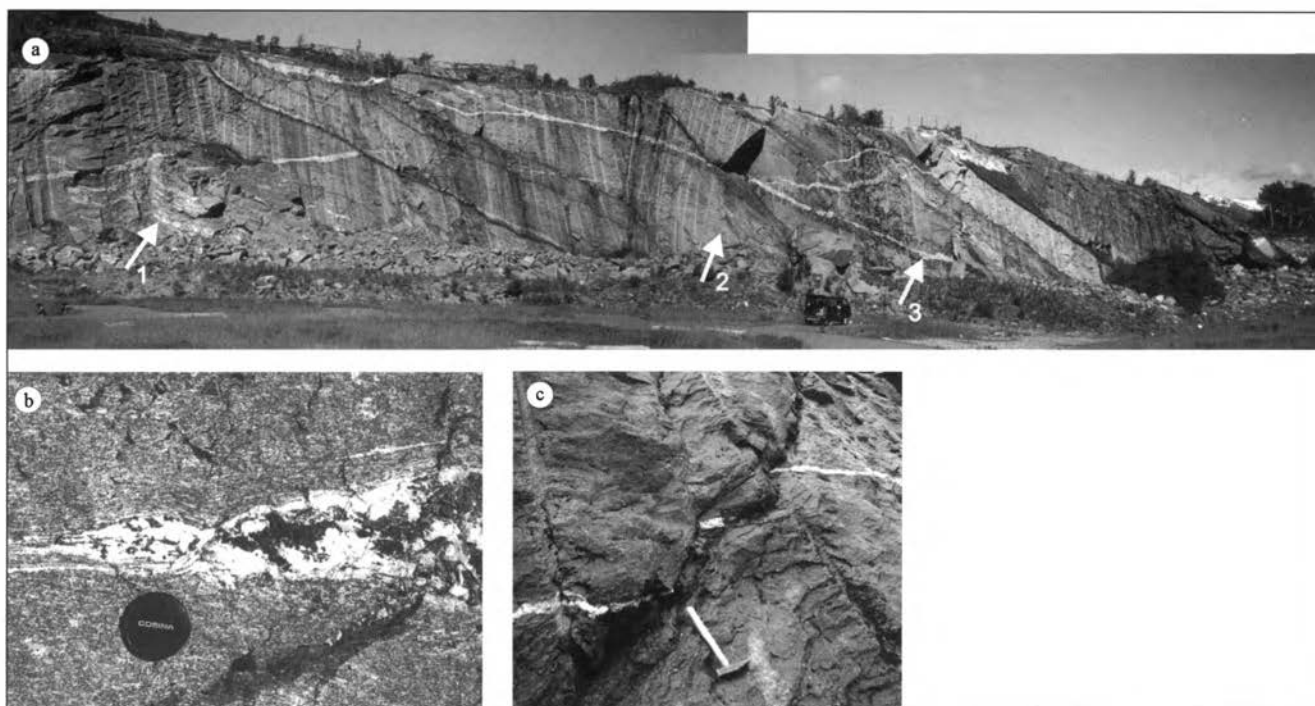


Fig. 4. Photographs showing important age relationships in the Sjona window: a) Overview of the roadside quarry described in the text, seen towards N. The pegmatite dykes are discordant to the gneiss foliation, but locally folded with axial surfaces parallel to the foliation. The arrows numbered 1-3 refer to the dated samples. See van for scale. b) Migmatitic neosome deformed into a layer parallel to the gneiss foliation. c) Retrograde, foliation-parallel extensional shear zone displacing a pegmatite in the quarry, seen towards NW. The dip of the shear plane and plunge of the striation (not visible) are towards the viewer. Note that steep lines on the picture are drill marks.

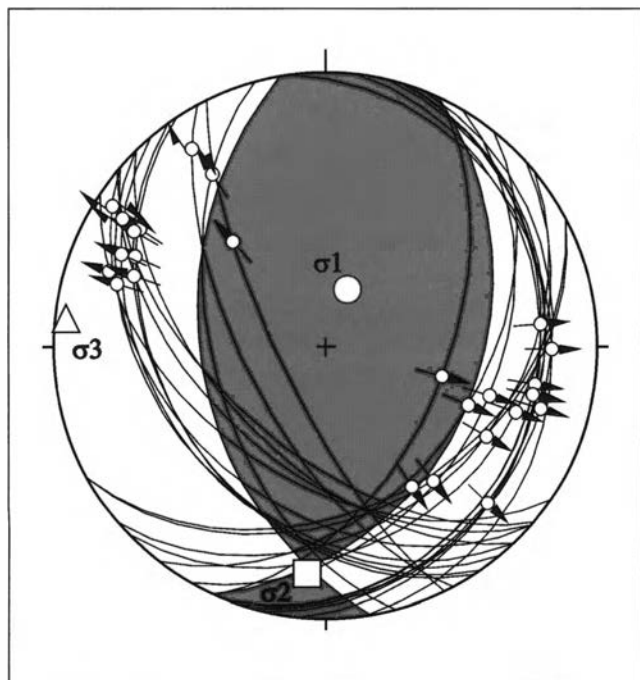


Fig. 5. Kinematic analysis based on the assumption that all of the measured semi-brittle to brittle shear zones have a component of normal-sense displacement. Arrows on the great circles represent striation measurements (also plotted in Fig. 2). The calculated maximum stress axis ( $\sigma_1$ ) is sub-vertical and the minimum stress axis ( $\sigma_3$ ) is E-W, presumably corresponding to the shortening and extension directions, respectively.

sic gneisses. The margins of the retrograde eclogite pods show a foliation concordant with the gneiss foliation indicating that the eclogitization predates the gneiss fabric.

Migmatitic gneisses on Træna comprise neosomes that are flattened parallel to the foliation in the adjacent gneiss, similar to migmatites in the Sjona window. The gneiss fabric therefore formed, at least partly, during and/or following this migmatization event. In the mafic rocks, pegmatites commonly crosscut the foliation. In contrast, in the surrounding gneiss most pegmatites are sub-parallel to the foliation, although some are seen to cut the foliation at high angles. Pegmatite emplacement also occurred in the necks of symmetric boudins that were stretched parallel to the gneiss foliation (Fig. 7a). These boudins, together with sporadic symmetric rootless folds with axial surfaces parallel to the foliation, are consistent with coaxial shortening normal to the foliation (sub-vertical). Asymmetric boudins and folds also exist, but no uniform shear directions could be ascribed to their development. Extensional shear bands associated with boudins cut the gneiss foliation, and define both symmetric and asymmetric geometries with easterly or westerly dip directions (Fig. 7b & c). Thus, a roughly E-W principal extension direction accompanies the sub-vertical shortening. The WNW-plunging lineation reported by Osmundsen et al. (in press) may relate to this extension. Coarse-grained biotite in the

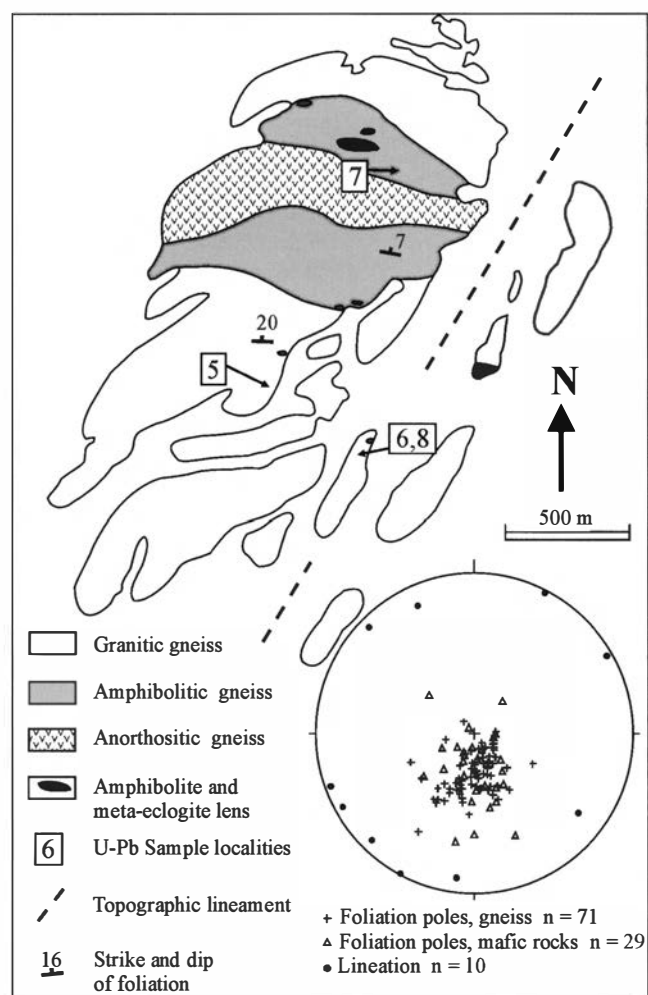


Fig. 6. Simplified geological map of the studied area on Træna (modified from Gustavson 1984 a, b) showing the locations of analysed U-Pb samples. The stereoplot (equal area lower hemisphere projection) shows the main gneiss foliation, the foliation in the mafic rocks, and a weakly developed lineation.

shear bands indicates that this extension did not involve significant retrograde metamorphism. In fact, mineral assemblages indicative of extensive retrograde conditions are only rarely observed in the gneisses on Træna, in contrast to the frequent observation of retrograde chlorite and sericite in the Sjøna window.

Despite the well-defined banding often seen at outcrop scale, the gneiss generally appears as weakly deformed at the microscale. At this scale, the foliation is predominantly defined by minor biotite and elongated amphibole and titanite, consistent with deformation under amphibolite-facies conditions. Quartz and feldspar show a granoblastic fabric (no preferred orientation), indicating that static recovery and recrystallization processes overprinted earlier fabrics in the gneiss. Such overprinting is a common feature in high-grade gneiss terranes (e.g. Passchier et al. 1990). Thus, the gneiss on Træna apparently resided at metamorphic conditions well within amphibolite-facies after the latest fabric development.

The gneiss foliation is cut by steep, brittle faults associated with several hydrothermal mineral phases, including epidote, chlorite, quartz and calcite, with minor amounts of titanite and white mica. Typically, the precipitation of these minerals resulted in wall-rock alteration, present as zones of anomalous red feldspar along the faults. Faults with these characteristics are observed within a pronounced NE-SW trending lineament in southern parts of the island (Fig. 6). Generally, the faults have trends around N-S and show normal-sense displacements. Although the number of observations is limited, this geometry is consistent with faulting under roughly E-W extension.

## U-Pb geochronology

The geological information provided by U-Pb dating of zircon and titanite from regional high-grade metamorphic rocks varies due to the different behaviour of these minerals (e.g. Frost et al. 2000). U-Pb zircon dating commonly provides information on original igneous crystallization events, although later metamorphic events and zircon overgrowth may also be reflected by the isotope system. Titanites on the other hand, are rather reactive since Ti- and Ca-rich mineral phases are present in most rocks. Since the closure temperature for diffusion of Pb in titanites (commonly regarded as ca. 660–700°C, Frost et al. 2000) often exceeds that of regional metamorphism, the U-Pb titanite ages often reflect metamorphic and deformation-related crystallization or recrystallization.

## Analytical techniques

Zircon and titanite were separated using standard mineral separation techniques. The zircons were abraded using the method described by Krogh (1982). All zircon and titanite fractions were washed in warm 4N HNO<sub>3</sub>, and rinsed in water and acetone prior to decomposition. Zircons and titanite were dissolved in HF and HNO<sub>3</sub> acids in Teflon bombs at 210°C and 160°C, respectively. A mixed <sup>205</sup>Pb/<sup>235</sup>U isotopic spike was added to the fractions prior to the dissolution. U and Pb were separated using standard anion-exchange techniques. Pb and U were loaded together with H<sub>3</sub>PO<sub>4</sub> and silica gel onto a rhenium filament and analysed on a Finnigan-MAT 262 thermal ionization mass spectrometer at the Department of Geology, University of Bergen. Measured isotopic ratios were corrected for mass fractionation by 0.1 % per AMU. Initial common Pb compositions were estimated using the Stacey and Kramers (1975) Pb evolution model (using an uncertainty of 1% on the <sup>207</sup>Pb/<sup>204</sup>Pb ratio of the corrected value.). Exceptions are initial common Pb compositions measured from K-feldspar. Errors on the ratios and ages correspond to 2σ.



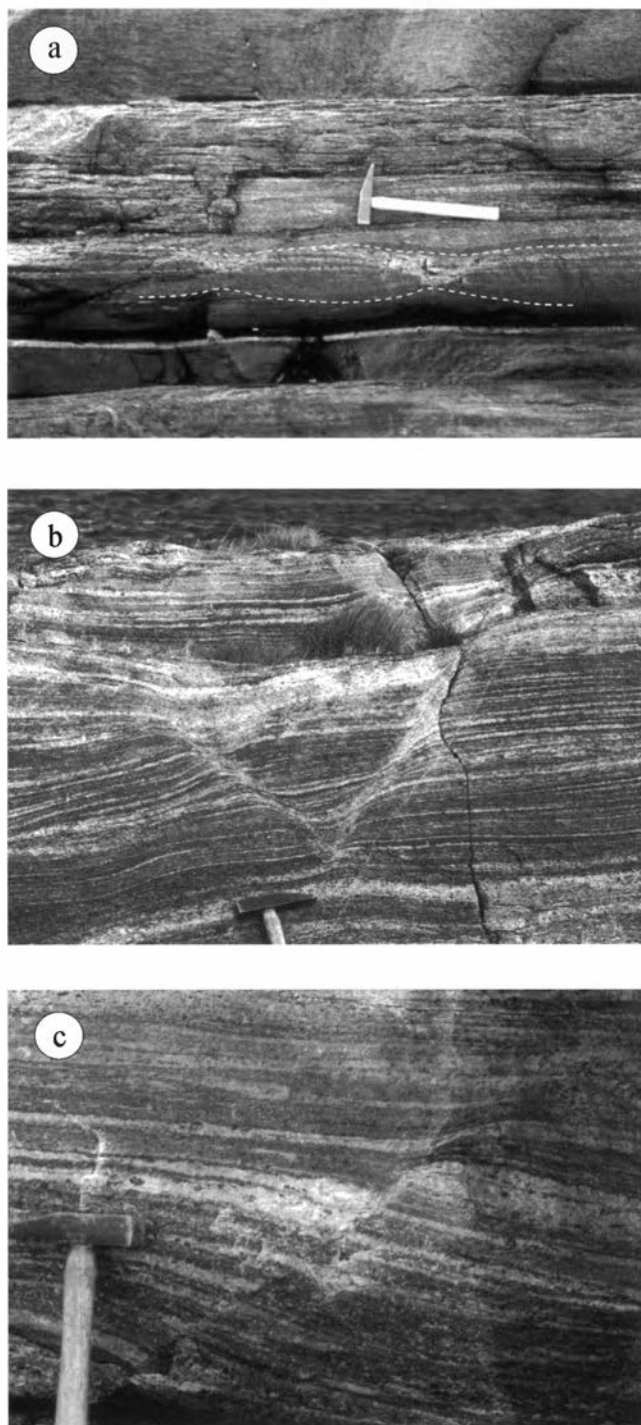


Fig. 7. a) Symmetric boudinage associated with pegmatite emplaced in the necks, seen towards N. b) Symmetric extensional shear bands defining a graben structure with east- and westward dip directions. c) Asymmetric extensional shear band dipping westward.

#### Sample description and analytical results

Eight samples have been dated in this study. Samples 1-3 were collected from a roadside quarry in southern parts of the Sjøna window (Fig. 4a), around 5 km west of the eastern nappe contact, whereas sample 4 is from the highly sheared mylonites at the eastern nappe contact. Samples 5-8 are from Træna. The locations of the dated samples are shown in Figs. 1 and 6.

#### The Sjøna window

**Sample 1 – Migmatite leucosomes** -- The granitic gneisses in the Sjøna window contain minor amounts of patch- and layered type migmatite. This sample was collected from the leucosome part of a migmatite that formed prior to, or during development of the foliation and top-to-the-E shearing (Fig. 4b). The leucosome is composed of K-feldspar, quartz and plagioclase, with minor amounts of biotite and hornblende. Epidote, apatite, titanite, zircon and oxides are accessory minerals. The melanosome of the migmatite occurs at the margin of, and as enclaves within the leucosome, and is composed of hornblende, biotite, epidote, titanite and oxides.

The zircons from the leucosome are pale brown and show prismatic and rounded shapes with a wide range of sizes. Most zircons have corroded surfaces, in contrast to zircons from the adjacent gneiss (Skår 2002). Three fractions of zircon were analysed (Table 1). These were free of inclusions and visible overgrowths, and define a discordia line with upper and lower intercepts of  $1797 \pm 3$  Ma and  $424 \pm 14$  Ma, respectively (Fig. 8a, Table 1).

**Sample 2 – Granitic gneiss** -- This sample was collected from the gneiss adjacent to the migmatite leucosome dated above (sample 1). The amphibolite-facies fabric of this sample, which affects the migmatite, is defined by plagioclase, K-feldspar, quartz, hornblende and biotite, with minor amounts of titanite, apatite, epidote, opaques and zircons. Titanites with grain sizes of 100-200  $\mu\text{m}$  (long axes) occur in relation to biotite and hornblende, and are aligned parallel to the foliation. Thus, the titanite crystallization (or recrystallization) is probably syn-kinematic with respect to the formation of the amphibolite-facies fabric.

In order to date this fabric, two fractions of inclusion free titanites were analysed (Table 1). These are 0.1 and 1.3% concordant, and yield  $^{206}\text{Pb}/^{238}\text{U}$  ages of  $425 \pm 3$  Ma and  $428 \pm 3$  Ma, respectively (Fig. 8a).

**Sample 3 – Discordant pegmatite** -- This large and weakly deformed pegmatite (Fig. 4a) postdates the amphibolite-facies fabric dated above (sample 2). The pegmatite is composed of K-feldspar, plagioclase and quartz with accessory biotite, pyrite and zircon. The zircons are usually dark brown, prismatic, metamict and rich in opaque inclusions.

The four zircon fractions that were analysed define a discordia line with an upper intercept of  $409 \pm 5$  Ma (Fig. 8b, Table 1). U-Pb dating of titanites contained in a pegmatite from western parts of the Svartisen window to the north (Fig. 1) yielded a consistent age of  $408 \pm 3$  Ma (Skår unpubl. data).

| Table 1. U/Pb data of zircon and titanite from the Sjøna window and Træna |                         |               |         |                         |                        |  |   |  |            |  |            |   |            |  |            |                |
|---|-------------------------|---------------|---------|-------------------------|------------------------|--|---|--|------------|--|------------|---|------------|--|------------|----------------|
| Fractions a)  |                         | Concentration |         |                         | Measured               | Atomic ratios c)                             |   |  |            | Ages (Ma)                                |            |   |            |  |            |                |
| No.   | Properties              | Weight (mg)   | U (ppm) | Pb <sub>rad</sub> (ppm) | Pb <sub>com</sub> (pg) | $\frac{^{206}\text{Pb(b)}}{^{204}\text{Pb}}$ | $\frac{^{208}\text{Pb}}{^{206}\text{Pb}}$ | $\frac{^{206}\text{Pb}}{^{238}\text{U}}$ | $\pm$ (2σ) | $\frac{^{207}\text{Pb}}{^{235}\text{U}}$ | $\pm$ (2σ) | $\frac{^{207}\text{Pb}}{^{206}\text{Pb}}$ | $\pm$ (2σ) | $\frac{^{206}\text{Pb}}{^{238}\text{U}}$ | $\pm$ (2σ) | Disc. d) (%)   |
| SJØNA WINDOW  |                         |               |         |                         |                        |  |   |  |            |  |            |   |            |  |            |                |
| Sample 1 Migmatite leucosome  |                         |               |         |                         |                        |  |   |  |            |  |            |   |            |  |            |                |
| Z1  | OM >100 lt br euh sp    | 0.069         | 133.1   | 43.3                    | 60                     | 2412   | 0.1663                                    | 0.29326                                  | 138        | 4.3865                                   | 242        | 0.10848                                   | 21         | 1658                                     | 7          | 1710 1774 7.4  |
| Z2  | OM 70–100 lt br euh sp  | 0.065         | 183.6   | 49.1                    | 78                     | 2053   | 0.1554                                    | 0.24342                                  | 120        | 3.5299                                   | 201        | 0.10517                                   | 20         | 1404                                     | 6          | 1534 1717 20.3 |
| Z3  | OM 30–70 lt br euh sp   | 0.060         | 189.9   | 41.4                    | 100                    | 1267   | 0.1555                                    | 0.19777                                  | 100        | 2.7468                                   | 166        | 0.10073                                   | 24         | 1163                                     | 5          | 1341 1638 31.6 |
| Sample 2 Granitic gneiss  |                         |               |         |                         |                        |  |   |  |            |  |            |   |            |  |            |                |
| T1  | lt br euh               | 0.427         | 78.5    | 9.0                     | 1718                   | 92   | 0.4139                                    | 0.06819                                  | 48         | 0.5203                                   | 214        | 0.05533                                   | 222        | 425                                      | 3          | 425 426 0.1    |
| T2  | lt br euh               | 0.512         | 54.1    | 6.6                     | 1616                   | 84   | 0.4559                                    | 0.06865                                  | 51         | 0.5256                                   | 245        | 0.05553                                   | 253        | 428                                      | 3          | 429 434 1.3    |
| Sample 3 Discordant pegmatite   |                         |               |         |                         |                        |  |   |  |            |  |            |   |            |  |            |                |
| Z4  | dk br fragm op incl met | 0.055         | 7393.0  | 412.0                   | 896                    | 1678   | 0.0264                                    | 0.05883                                  | 40         | 0.4479                                   | 35         | 0.05522                                   | 15         | 368                                      | 2          | 376 421 12.9   |
| Z5  | dk br euh lp op incl    | 0.005         | 8033.1  | 495.0                   | 81                     | 1977   | 0.0260                                    | 0.06531                                  | 43         | 0.4958                                   | 38         | 0.05506                                   | 16         | 408                                      | 3          | 409 410 0.5    |
| Z6  | dk br fragm op incl met | 0.044         | 5980.6  | 348.5                   | 447                    | 2250   | 0.0199                                    | 0.06221                                  | 29         | 0.4718                                   | 27         | 0.05501                                   | 14         | 389                                      | 2          | 392 413 5.9    |
| Z7  | dk br fragm op incl met | 0.016         | 5586.3  | 360.2                   | 559                    | 651  | 0.0622                                    | 0.06401                                  | 30         | 0.4859                                   | 38         | 0.05505                                   | 31         | 400                                      | 2          | 402 414 3.6    |
| Sample 4 Mylonitic gneiss   |                         |               |         |                         |                        |  |   |  |            |  |            |   |            |  |            |                |
| T3  | lt br fragm             | 0.287         | 179.6   | 17.7                    | 1826                   | 127  | 0.3012                                    | 0.06819                                  | 40         | 0.5260                                   | 150        | 0.05595                                   | 153        | 425                                      | 2          | 429 450 5.8    |
| T4  | lt br fragm             | 0.338         | 200.4   | 19.4                    | 2284                   | 132  | 0.2939                                    | 0.06805                                  | 37         | 0.5396                                   | 144        | 0.05751                                   | 147        | 425                                      | 2          | 438 511 17.6   |
| TRÆNA   |                         |               |         |                         |                        |  |   |  |            |  |            |   |            |  |            |                |
| Sample 5 Granitic gneiss  |                         |               |         |                         |                        |  |   |  |            |  |            |   |            |  |            |                |
| T5  | lt br euh + fragm       | 0.307         | 55.3    | 13.4                    | 2885                   | 39   | 1.0388                                    | 0.06793                                  | 100        | 0.5176                                   | 685        | 0.05526                                   | 726        | 424                                      | 6          | 424 423 -0.2   |
| Sample 6 Migmatite leucosome  |                         |               |         |                         |                        |  |   |  |            |  |            |   |            |  |            |                |
| T6  | 10mm dk br euh          | 0.379         | 200.3   | 15.6                    | 1223                   | 243  | 0.2222                                    | 0.06355                                  | 36         | 0.4782                                   | 75         | 0.05458                                   | 76         | 397                                      | 2          | 397 395 0.6    |
| T7  | 10mm dk br euh          | 0.400         | 196.8   | 15.5                    | 1308                   | 237  | 0.2229                                    | 0.06369                                  | 41         | 0.4799                                   | 79         | 0.05465                                   | 81         | 398                                      | 2          | 398 398 0.0    |
| T8  | 10mm dk br euh          | 0.305         | 198.1   | 15.4                    | 946                    | 249  | 0.2168                                    | 0.06366                                  | 36         | 0.4798                                   | 77         | 0.05466                                   | 79         | 398                                      | 2          | 398 398 0.1    |
| Sample 7 Discordant pegmatite e)  |                         |               |         |                         |                        |  |   |  |            |  |            |   |            |  |            |                |
| T9  | 10mm lt br euh          | 0.371         | 16.8    | 2.6                     | 478                    | 67   | 0.8092                                    | 0.06450                                  | 59         | 0.5077                                   | 308        | 0.05709                                   | 341        | 403                                      | 4          | 417 495 18.0   |
| T10   | 10mm lt br euh          | 0.512         | 14.7    | 2.1                     | 501                    | 74   | 0.7694                                    | 0.06447                                  | 52         | 0.4934                                   | 269        | 0.05550                                   | 298        | 403                                      | 3          | 407 433 7.0    |
| Sample 8 Fault-related titanite f)  |                         |               |         |                         |                        |  |   |  |            |  |            |   |            |  |            |                |
| T11   | lt br euh               | 0.587         | 12.4    | 2.9                     | 1351                   | 36   | 1.0205                                    | 0.05851                                  | 112        | 0.4240                                   | 734        | 0.05256                                   | 899        | 367                                      | 7          | 359 310 -19.0  |
| T12   | lt br euh               | 0.525         | 17.2    | 3.3                     | 1237                   | 42   | 0.8628                                    | 0.05876                                  | 87         | 0.4372                                   | 551        | 0.05397                                   | 674        | 368                                      | 5          | 368 370 0.5    |
| T13   | lt br euh               | 0.490         | 18.8    | 3.3                     | 1116                   | 45   | 0.7998                                    | 0.05876                                  | 82         | 0.4376                                   | 488        | 0.05402                                   | 632        | 368                                      | 5          | 369 372 1.0    |

Table captions: <sup>a</sup> Abbreviations are: T = titanite; Z = zircon; 30–100 = mineral size (mm); br = brown; dk = dark; lt = light; euh = euhedral; sp = short prism; lp = long prism; fragm = fragment; met = metamict; op incl = opaque inclusions. <sup>b</sup> Corrected for fractionation and common lead in spike. <sup>c</sup> Corrected for fractionation and spike, lab Pb blank of 5–15 pg (zircon), 30 pg (titanite), initial common Pb calculated from the model of Stacey & Kramers (1975) and 2 pg U blank. <sup>d</sup> % discordance of the fraction from concordia curve on a chord through the origin. <sup>e</sup> Common Pb corrected by K-feldspar from the pegmatite with Pb isotopic composition:  $^{206}\text{Pb}/^{204}\text{Pb} = 16.520$ ,  $^{207}\text{Pb}/^{204}\text{Pb} = 15.327$ ,  $^{206}\text{Pb}/^{204}\text{Pb} = 35.940$ . <sup>f</sup> Common Pb corrected by K-feldspar from the wall rock with Pb isotopic composition:  $^{206}\text{Pb}/^{204}\text{Pb} = 16.534$ ,  $^{207}\text{Pb}/^{204}\text{Pb} = 15.313$ ,  $^{208}\text{Pb}/^{204}\text{Pb} = 35.813$ .



**Sample 4 – Mylonitic gneiss** -- The mylonitic top-to-the-E fabric of this sample, taken from the eastern nappe contact, is defined by K-feldspar, plagioclase, quartz, and biotite. Accessory minerals are titanite, apatite, epidote, zircon and opaques. The titanites are often associated with biotite, and occur as anhedral, elongated grains with their long axes (200–500  $\mu\text{m}$ ) aligned parallel to the foliation. Also, some titanites occur as aggregates in foliation-parallel trains. These relationships suggest that the titanite crystallization (or recrystallization) was syn-kinematic with respect to the fabric formation.

Two fractions of titanites from this sample were analysed, both yielding  $^{206}\text{Pb}/^{238}\text{U}$  ages of  $425 \pm 2$  Ma (Fig. 8c, Table 1).

#### Interpretation of sample 1–4

The presence of melanosome together with leucosome in sample 1 shows that the migmatite formed by in situ partial melting of the adjacent gneiss (Sample 2). The corroded surfaces of zircons from the leucosome and larger discordance on the concordia diagram relative to zircons from sample 2 (Skår 2002) suggest that the former zircons suffered dissolution-related Pb-loss. Thus, the lower intercept age at  $424 \pm 14$  Ma is interpreted to date migmatization. The upper intercept age is interpreted as the crystallization age for the adjacent gneiss protolith (Skår 2002).

U/Pb analyses of metamorphic titanites yielded ages of  $425 \pm 3$  Ma and  $428 \pm 3$  Ma in sample 2, and  $425 \pm 2$  Ma for two fractions in sample 4. These ages are interpreted in terms of syn-tectonic mineral growth associated with development of the amphibolite-facies fabric and top-to-the-E shearing. It is therefore likely that the mean age (c. 425 Ma), consistent with the migmatization age discussed above, is related to the Scandian nappe emplacement.

The upper intercept age of  $409 \pm 5$  Ma obtained from zircons in the discordant pegmatite (sample 3) is interpreted to date a phase of pegmatite emplacement. Based on field relations, this age also constrains the age of a late ductile deformation phase in the Sjøna window, which is likely to be related to the dome formation.

#### Træna

**Sample 5 – Granitic gneiss** -- This sample represents the amphibolite-facies gneiss on Træna, of which the major constituents are K-feldspar, plagioclase, quartz, biotite and hornblende. Accessory minerals are titanite, epidote, apatite, zircons and opaques. Relatively large grains of subhedral to anhedral titanite, commonly associated with hornblende and biotite, occur with

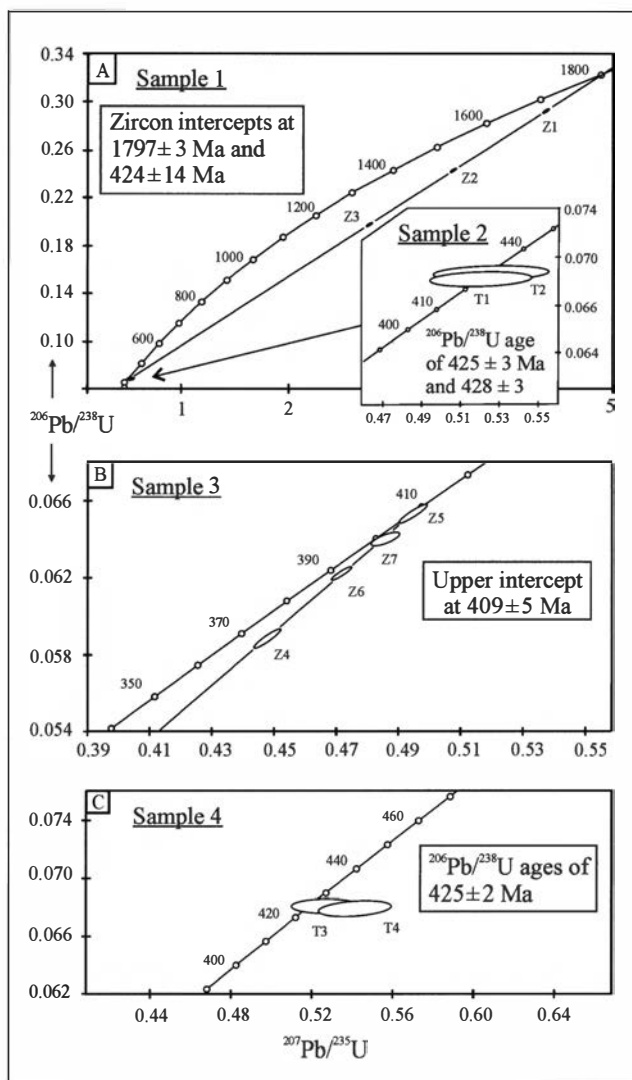


Fig. 8. Concordia diagram for zircon and titanite from the Sjøna window. See text for details.

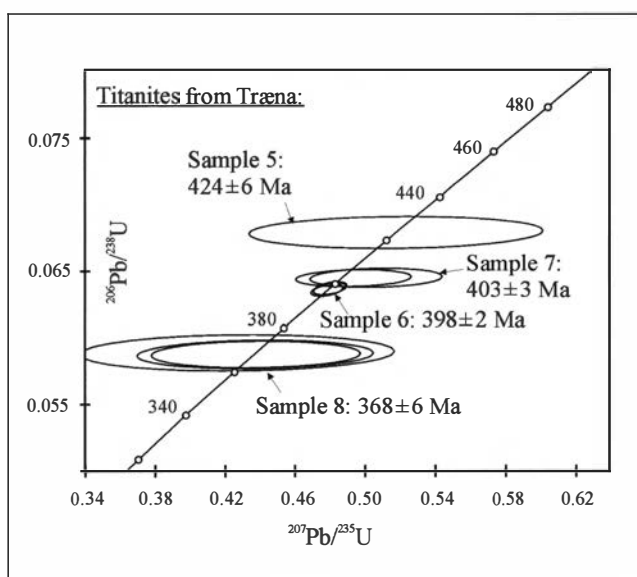


Fig. 9. Concordia diagram for titanites from Træna. See text for details.

their long axes (300–1000  $\mu\text{m}$ ) parallel to the gneiss fabric. Thus, a genetic relationship appears to exist between the amphibolite-facies fabric and titanite (re)crystallization.

A fraction of light brown fragments of titanite grains was analysed (Table 1). The fraction yielded a concordant  $^{206}\text{Pb}/^{238}\text{U}$  age of  $424 \pm 6$  Ma (Fig. 9).

*Sample 6 – Migmatite neosome* -- This sample was collected from a 0.5 m long and 5 cm thick migmatite leucosome in the southern parts of Træna (Fig. 6). The major constituents of the leucosome are plagioclase, K-feldspar and quartz with minor amounts of biotite and hornblende. Accessory titanite occurs as large, euhedral crystals in textural equilibrium with these minerals. The melanosome part of the migmatites is composed of hornblende in enclaves within the leucosome and more rarely along the margins of the leucosomes. The neosome is flattened parallel to the surrounding gneiss foliation, and thus represents an important time marker.

Three fractions of a single, 10-mm long, dark brown titanite crystal were analysed (Table 1). These yielded high U-values (196–200 ppm) and concordant  $^{206}\text{Pb}/^{238}\text{U}$  ages of  $398 \pm 2$  Ma (Fig. 9). A lower intercept age of  $392 \pm 13$  Ma yielded by three zircon fractions from the protolith of the migmatite is in agreement with this age (Skår 2002).

*Sample 7 – Discordant pegmatite* -- Sample 7 was collected from a discordant pegmatite in the anorthositic rocks in central parts of Træna. The sample is composed of plagioclase, K-feldspar and quartz, and contains accessory amounts of clinopyroxene (partly altered to amphibole) and titanite.

Two fractions of a single 10 mm long, euhedral, and light brown titanite with no inclusions were analysed (Table 1). Initial common lead composition was measured in coexisting K-feldspar. The titanite fractions are concordant within error, and yield an  $^{206}\text{Pb}/^{238}\text{U}$  age of  $403 \pm 3$  Ma (Fig. 9).

*Sample 8 – Fault-related titanite* -- Polished and striated normal faults associated with epidote, chlorite, and quartz also contain minor amounts of co-genetic titanite and white mica. Some of the titanites form large (2–10 mm), euhedral crystals.

Three fractions taken from a single, 8 mm long, pale brown titanite were analysed (Table 1). They have an U content of about 15 ppm, and yielded concordant  $^{206}\text{Pb}/^{238}\text{U}$  ages with a mean age of  $368 \pm 6$  Ma (Fig. 9). Initial common lead composition was constrained by analyses of K-feldspar from the hydrothermally altered wall rock close to the fault plane.

*Interpretation of samples 5–8* -- The U/Pb analysis of metamorphic titanite in sample 5 yielded an age of  $424 \pm 6$  Ma, which is interpreted to date syn-kinematic titanite growth during fabric development in the gneiss. This age is similar to the Scandian ages yielded by metamorphic titanites in the Sjøna window, indicating that both areas were affected by regional metamorphism at that time.

Melanosome associated with leucosome in the migmatite of sample 6 demonstrates in situ partial melting. A relatively large titanite from the leucosome was dated to  $398 \pm 2$  Ma. The size of this titanite is significantly larger than concordant titanites in sample 5. Thus, if the age of the large titanite reflected isotopic resetting, it would be expected that titanites in sample 5 also were affected. This is not the case, and the age of  $398 \pm 2$  Ma is therefore interpreted to date the migmatization event.

A relatively large titanite in the pegmatite of sample 7 yielded an age of  $403 \pm 3$  Ma, overlapping with the migmatization event dated above. Following the same argument as above, the large grain size relative to titanites in sample 5 indicates that this age reflects titanite growth related to pegmatite emplacement.

A euhedral titanite on the polished surfaces of a N-S trending normal fault (sample 8) yielded an age of  $368 \pm 6$  Ma, which is interpreted to date titanite growth from hydrothermal fluids circulating along the fault. Furthermore, the association with fault-related minerals suggests that this age also closely corresponds to the age of the normal faulting.

## Discussion

### *Scandian nappe emplacement*

The early tectono-thermal event recognised in both the Sjøna window and on Træna at around 425 Ma is related to regional metamorphism. In the Sjøna window, this event involved local migmatite formation associated with ductile top-to-the-E shearing in areas close to the eastern nappe contact. Thus, the Silurian age in this area seems to be related to Scandian eastward thrusting of the Uppermost Allochthon, and is in agreement with the youngest pre-Scandian intrusions that were emplaced in more southerly parts of the HNC at around 430 Ma (Nordgulen et al. 1993). Similarly, thrusting and regional metamorphism of the Uppermost Allochthon took place at around, and after 430 Ma in the Ofoten area to the north (Coker et al. 1995; Northrup 1997).

Scandian metamorphism at around 425 Ma is also recorded on Træna, but structures that consistently reflect east-directed thrusting were not identified. A

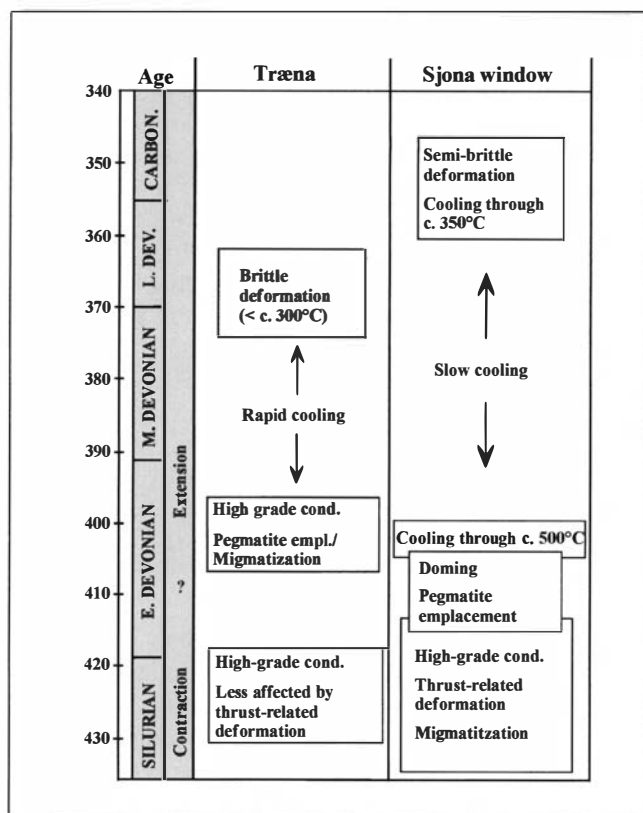


Fig. 10. Timetable showing the tectono-thermal evolution of Træna and the Sjøna window. See text for details.

reason for this may be that thrust-related deformation was either weak and/or overprinted by a later structural and thermal event. The latter alternative is considered likely seen in light of the migmatization and pegmatite emplacement recorded at around 400 Ma, and indications of late recovery/recrystallization processes in the gneiss. Moreover, in contrast to the Sjøna window, which is situated in direct contact with the overlying allochthons, the gneisses on Træna may have resided at a crustal level that was weakly affected by the nappe emplacement. Different crustal levels for the two areas are also supported by the occurrence of retrograde eclogites on Træna, but not on the mainland.

### Dome formation

Gneiss-cored culminations are common features along the Caledonides of central and north Norway (Fig. 1), and several tectonic models have been proposed to explain their formation. In broad terms, these models involve doming due to contractional nappe stacking (Greiling et al. 1993), gravitational tectonics (Ramberg 1980; Cooper & Bradshaw 1980; Speedyman 1989), or extensional tectonics (Rykkeliid & Andresen 1994; Osmundsen et al. in press).

The sub-circular dome exposed in the Sjøna window probably formed during and/or after Scandian thrust-

ting since the overlying allochthon was also affected. It is likely that the roughly radial pattern of the lineation and associated shear-sense indicators, inferred to overprint pegmatites emplaced at around 409 Ma, reflects this dome formation. Furthermore, the top-to-the-SW shearing in the southwest is not compatible with the general eastward thrust direction in the Caledonides. Thus, a model in which the doming was due to contractional nappe stacking seems unlikely, contrary to what has been inferred in the eastern foreland region of the Caledonides (Greiling et al. 1993).

More likely, the radial pattern reflects doming due to uplift of the gneisses, related to gravitational tectonics (diapirism) and/or extensional tectonics (footwall uplift along the NSZ). In such a scenario, pegmatite emplacement at around 409 Ma may be related to decompression melting, and the  $^{40}\text{Ar}/^{39}\text{Ar}$  amphibole ages of 418–401 Ma (Dallmeyer 1988) can be taken to reflect associated cooling. Gravitational tectonics has been suggested to be important in the formation of gneiss-cored culminations 150–200 km north of the present study area (Ramberg 1980; Cooper & Bradshaw 1980; Speedyman 1989). According to these workers, the emplacement of relatively dense nappes onto light granitic gneisses in association with regional high-grade metamorphism triggered gravitational adjustment and doming. Similarly, a gravitational process could have contributed to the dome formation in the Sjøna window, since the nappe emplacement there most likely caused an inverted density contrast. Alternatively or additionally, the dome formation in the Sjøna window was influenced by footwall uplift during extensional shearing on the NSZ (Osmundsen et al. in press). The top-to-the-SW sense of shear in the southwestern part of the Sjøna window may be related to displacement along the overlying NSZ, implying that the suggested Early Devonian age of doming also dates extensional deformation in the area. It is possible that U/Pb titanite ages of 401–386 Ma, reported from the western Nasafjället window (Fig. 1, Essex & Gromet 2000), date extensional deformation similar to that associated with the NSZ (Osmundsen et al. in press). Furthermore, uplift of the Rombak window in the Ofoten area (Fig. 1) is inferred to be a result of extensional top-to-the-W shearing along the western margin of the window (Fossen & Rykkeliid 1992; Rykkeliid & Andresen 1994). In this area, however, the extensional displacement is confined to 371–355 Ma by  $^{40}\text{Ar}/^{39}\text{Ar}$  biotite and muscovite dating (Coates et al. 1999), and is thus younger than the doming in the Sjøna window and the shearing along the NSZ.

### Differential exhumation

The gneiss fabric on Træna partly developed during Scandian deformation and metamorphism at around

425 Ma, as discussed above. However, ductile flattening of a migmatite neosome dated to  $398 \pm 2$  Ma and pegmatite emplacement at around  $403 \pm 3$  Ma indicate that the gneiss fabric also was influenced by a later tectono-thermal stage in the Early Devonian. This stage likely affected the whole region, since the pegmatite age on Træna broadly conforms to dated pegmatites on the mainland;  $409 \pm 5$  Ma in the Sjana window (this study) and  $408 \pm 3$  Ma in the Svartisen window (Skår, unpubl. data). The Early Devonian pegmatites and migmatites on Træna are interpreted to result from decompression melting during uplift of the gneisses. The required crustal temperature to allow for such partial melting is at least  $650^\circ\text{C}$  (Bucher and Frey 1994). Partial melting is also recorded in the Sjana window by pegmatite emplacement at  $409 \pm 5$  Ma. However,  $^{40}\text{Ar}/^{39}\text{Ar}$  dating from the same area (Dallmeyer 1988) indicates that the temperature had decreased to around  $500^\circ\text{C}$  at around 401 Ma (Fig. 10). The late-stage ductile deformation on Træna is interpreted in terms of bulk coaxial strain with sub-vertical shortening and roughly E-W extension, contrary to the non-coaxial deformation in the Sjana window and the overlying NSZ. This contrast in temperature and deformation suggests that the rocks on Træna were situated at a lower crustal level than their mainland equivalents, as suggested above for Silurian time.

U/Pb dating of titanites associated with faults on Træna ( $368 \pm 6$  Ma) indicates that the gneisses had entered the brittle regime ( $<300^\circ\text{C}$ ) by the Middle-Late Devonian (Fig. 10). Although no comprehensive structural study of these faults has been carried out, they suggest E-W extension, which is compatible with the extension direction inferred from semi-brittle to brittle shear zones in the Sjana window. The formation of these shear zones is not directly constrained by absolute age determinations. However, the greenschist-facies metamorphism associated with these structures suggests them to be active at temperatures attained during the Middle Devonian to Early Carboniferous, as indicated by Rb/Sr biotite dating (Wilberg 1987) and  $^{40}\text{Ar}/^{39}\text{Ar}$  dating of biotite (Eide et al. in review). The above time considerations suggest that differential exhumation had brought the rocks on Træna to comparable crustal levels as their mainland equivalents by the Middle-Late Devonian (Fig. 10).

## Conclusions

The following main conclusions on the tectonic history of the Sjana window and Træna have been made based on U-Pb geochronology combined with structural and petrologic investigations:

1. Scandian east-directed thrusting and regional high-grade metamorphism occurred at around 425 Ma. At

the crustal levels presently exposed on Træna, this event did not significantly affect the structural development, but is recorded by metamorphic titanite growth in the gneiss. In contrast, the structural development in the southern parts of the Sjana window appears to be more influenced by this thrusting.

2. The Sjana window and the overlying allochthon developed into a sub-circular dome during and/or following the Scandian nappe emplacement. The dome formation persisted at least into the Early Devonian, and probably involved vertical uplift of the gneisses. Two dome-forming processes are considered likely; gravitational (diapiric) adjustment caused by an inverted density contrast between the gneisses of the Sjana window and the overlying allochthon, or footwall uplift due to extensional deformation along the NSZ, or a combination of these processes.

3. The rocks on Træna were subjected to high-grade conditions ( $>650^\circ\text{C}$ ) associated with migmatization and pegmatite emplacement at around 400 Ma. At the same time, the rocks of the Sjana window cooled through temperatures of ca.  $500^\circ\text{C}$ , consistent with the two areas being situated at different crustal levels.

4. During the Middle-Late Devonian, the rocks on Træna and in the Sjana window reached approximately the same crustal level (semi-brittle to brittle regime) as a result of differential exhumation.

*Acknowledgements.* – This paper is part of the first author's PhD work. We are thankful to P. T. Osmundsen, A. Andresen and H. Fossen for constructive suggestions and comments on an early version of the paper. Comments from the referees (E. Rehnström, F. Corfu and P. T. Osmundsen) are also acknowledged. Elizabeth Eide is thanked for correcting the language. The Norwegian Research Council and the BAT research program at the Norwegian Geological Survey have supported this work.

## References

- Andersen, T.B. & Jamtveit, B. 1990: Uplift of deep crust during orogen extensional collapse: A model based on field studies in the Sogn-Sunnfjord region of western Norway. *Tectonics* 9, 1097-1111.
- Bucher, K. & Frey, M. 1994: *Petrogenesis of Metamorphic Rocks*. Springer-Verlag, Berlin. 318pp.
- Coates, B.H., Zeltner, D.L., Carter, B.T., Steltenpohl, M.G., Andresen, A. & Kunk, M.J. 1999:  $^{40}\text{Ar}/^{39}\text{Ar}$  and structural investigations of extensional development of the North-Central Norwegian margin. *Abstracts with programs, Geological Society of America* 31, 118.
- Coker, J.E., Steltenpohl, M.G., Andresen, A. & Kunk, M.J. 1995: An  $^{40}\text{Ar}/^{39}\text{Ar}$  thermochronology of the Ofoten-Troms region: Implications for terrain amalgamation and extensional collapse of the northern Scandinavian Caledonides. *Tectonics* 14, 435-447.
- Cooper, M.A. & Bradshaw, R. 1980: The significance of basement gneiss domes in the tectonic evolution of the Salta Region, Norway. *Journal of the Geological Society, London* 137, 231-240.
- Eide, E.A., Osmundsen, P.T., Meyer, G.B., Kendrick, M.A. & Corfu, F. 2002: The Nesna Shear Zone, north-central Norway: an  $^{40}\text{Ar}/^{39}\text{Ar}$  record of Early Devonian – Early Carboniferous ductile extension and unroofing. *Norsk Geologisk Tidsskrift*, in press.
- Essex, R.M. & Gromet, L.P. 2000: U-Pb dating of prograde and retrograde titanite growth during the Scandian orogeny. *Geology* 28, 419-422.
- Dallmeyer, R.D. 1988: Polyphase tectonothermal evolution of the Scandinavian Caledonides. In Harris, A.L. & Fettes, D.J. (eds.) *The Caledonian-Appalachian Orogen*. Geological Society Special Publication 38, 365-379.
- Fossen, H. 1992: The role of extensional tectonics in the Caledonides of south Norway. *Journal of Structural Geology* 14, 1033-1046.
- Fossen, H. & Rykkelid, E. 1992: Postcollisional extension of the Caledonide orogen in Scandinavia: Structural expressions and tectonic significance. *Geology* 20, 737-740.
- Fossen, H. & Dunlap, W.J. 1998: Timing and kinematics of Caledonian thrusting and extensional collapse, southern Norway: evidence from  $^{40}\text{Ar}/^{39}\text{Ar}$  thermochronology. *Journal of Structural Geology* 20, 765-781.
- Frost, B.R., Chamberlain, K.R. & Schumacher, J.C. 2000: Sphene (titanite): phase relations and role as a geochronometer. *Chemical Geology* 172, 131-148.
- Gee, D.G. 1975: A tectonic model for the central part of the Scandinavian Caledonides. *American Journal of Science* 275-A, 468-515.
- Greiling, R.O., Gayer, R.A. & Stephens, M.B. 1993: A basement culmination in the Scandinavian Caledonides formed by antiformal stacking (Bångonåve, northern Sweden). *Geological Magazine* 130, 471-482.
- Gustavson, M. 1984a: Træna Fyr. Foreløpig berggrunnskart 1727 I, 1: 50 000, Norges geologiske undersøkelse.
- Gustavson, M. 1984b: Træna. Foreløpig berggrunnskart 1728 II, 1: 50 000, Norges geologiske undersøkelse.
- Gustavson, M. & Gjelle, S.T. 1991: Mo i Rana. Berggrunnsgeologisk kart, 1:250000, Norges geologiske undersøkelse.
- Klein, A.C. & Steltenpohl, M.G. 1999: Basement-cover relations and late- to post-Caledonian extension in the Leknes group, west-central Vestvågøy, Lofoten, north Norway. *Norsk Geologisk Tidsskrift* 79, 19-31.
- Klein, A.C., Steltenpohl, M.G., Hames, W.E. & Andresen, A. 1999: Ductile and brittle deformation in the southern Lofoten archipelago, north Norway: Implications for differences in tectonic style along an ancient collisional margin. *American Journal of Science* 299, 69-89.
- Krogh, E.J. 1980: Geochemistry and petrology of glaucophane-bearing eclogites and associated rocks from Sunnfjord, western Norway. *Lithos* 13, 355-380.
- Krogh, T.E. 1982: Improved accuracy of U-Pb zircon ages by the creation of more concordant systems using an air abrasion technique. *Geochimica et Cosmochimica Acta* 46, 637-649.
- Milnes, A.G., Wennberg, O.P., Skår, Ø. & Koestler, A.G. 1997: Contraction, extension and timing in the south Norwegian Caledonides-the Sognefjord transect. In Burg, J. P. & Ford, M. (eds.) *Orogeny through time*. Geological Society of London, Special Publication 121, 123-148.
- Nordgulen, Ø., Bickford, M.E., Nissen, A.L. & Wortman, G.L. 1993: U-Pb zircon ages from the Bindal Batholith, and the tectonic history of the Helgeland Nappe Complex, Scandinavian Caledonides. *Journal of the Geological Society, London* 150, 771-783.
- Northrup, C.J. 1996: Structural expression and tectonic implications of general noncoaxial flow in the midcrust of a collisional orogen: The northern Scandinavian Caledonides. *Tectonics* 15, 490-505.
- Northrup, C.J. 1997: Timing, structural assembly, metamorphism, and cooling of Caledonian nappes in the Ofoten-Esfjorden area, North Norway: tectonic insights from U-Pb and  $^{40}\text{Ar}/^{39}\text{Ar}$  geochronology. *Journal of Geology* 105, 565-582.
- Osmundsen, P.T., Braathen, A., Nordgulen, Ø., Roberts, D., Meyer, G.B. & Eide, E. 2002: The Devonian Nesna Shear Zone and adjacent gneiss-cored culminations, north-central Norwegian Caledonides. *Journal of the Geological Society, London* (in press).
- Passchier, C.W., Myers, J.S. & Kröner, A. 1990: *Field geology of high-grade gneiss terrains*. Springer-Verlag, 150pp.
- Ramberg, H. 1980: Diapirism and gravity collapse in the Scandinavian Caledonides. *Journal of the Geological Society, London* 137, 261-270.
- Roberts, D. & Gee, D.G. 1985: An introduction to the structure of the Scandinavian Caledonides. In Gee, D. G. & Sturt, B. A. (eds.) *The Caledonide Orogen-Scandinavia and related areas*, 55-68. Wiley, Chichester.
- Rykkelid, E. & Andresen, A. 1994: Late Caledonian extension in the Ofoten area, northern Norway. *Tectonophysics* 231, 157-169.
- Skår, Ø. 2002: U-Pb geochronology and geochemistry of early Proterozoic rocks of the tectonic basement windows in central Nordland, Caledonides of north-central Norway. *Precambrian Research* 116, 265-283.
- Speedyman, D.L. 1989: Basement gneiss doming in the Uppermost Allochthon in the Bogøy area of Steigen, Nordland, Norway. *Norges geologiske undersøkelse, Bulletin* 414, 37-47.
- Stacey, J.S. & Kramers, J.D. 1975: Approximation of terrestrial lead isotope evolution by a two-stage model. *Earth and Planetary Science Letters* 26, 207-221.
- Steiger, R.H. and Jäger, E. 1977: Subcommission on Geochronology: Convention on the use of decay constants in geo- and cosmochronology. *Earth Planetary Science Letters* 36, 359-362.
- Stephens, M.B., Gustavson, M., Ramberg, I.B. & Zachrisson, E. 1985: The Caledonides of central-north Scandinavia-a tectonostratigraphic overview. In Gee, D. G. & Sturt, B. A. (eds.) *The Caledonide Orogen-Scandinavia and related areas*, 135-162. Wiley, Chichester.
- Wilberg, R. 1987: Rekognoserende Rb-Sr alderbestemmelser av granitiske gneiser fra grunnfjellsvinduene Høgtuva og Sjøna i Nordland. *Norges geologiske undersøkelse, report* 87.074, 21 pp.
- Wilson, M.R. & Nicholson, R. 1973: The structural setting and geochronology of basal granitic gneisses in the Caledonides of part of Nordland, Norway. *Journal of the Geological Society, London* 129, 365-387.